Diffusion behaviour of cesium in silicon carbide at T > 1000 °C

E. Friedland[(a)*], N.G. van der Berg[(a)], T.T. Hlatshwayo[(a)], R.J. Kuhudzai[(a)],
J.B. Malherbe[(a)], E. Wendler[(b)], W. Wesch[(b)]

[(a)]Physics Department, University of Pretoria, Pretoria, South Africa

[(b)]Institut für Festkörperphysik, Friedrich-Schiller-Universität, Jena, Germany

Abstract.

Diffusion behaviour of ion implanted cesium into 6H-SiC and CVD-SiC wafers is investigated by Rutherford backscattering spectrometry (RBS) combined with α-particle channelling and scanning electron microscopy (SEM). Implantations were done at room temperature, 350 °C and 600 °C. A strong temperature dependence of irradiation induced diffusion is observed. Transport mechanisms were studied by isochronal and isothermal annealing methods up to temperatures of 1500 °C. Cesium transport in irradiation damaged SiC is governed by an impurity trapping mechanism of defect structures and is similar in single and polycrystalline SiC.

Keywords: Diffusion, Silicon Carbide, Ion implantation. Isochronal and Isothermal Annealing.

1. Introduction

Fuel elements of modern high-temperature nuclear reactor (HTR) designs commonly contain TRISO fuel particles, which consist of fuel kernels encapsulated by CVD-layers of low and high density pyrolitic carbon and silicon carbide. In these fuel particles the silicon carbide coating is the main barrier to limit fission product release into the primary cooling gas circuit. Up to temperatures of about 1000 °C reached in formerly and currently operating gas cooled reactors, release of fission products from fuel particles during their total resident time in the core is fairly low [1]. To further enhance the efficiency of HTR's, especially in view of their possible use as a heat source for the hydrogen energy technology [2], some advanced design studies envisage operating temperatures significantly above 1000 °C. However, as little information on diffusion behaviour of fission products through silicon carbide is available for this temperature region, we are pursuing a systematic study of diffusion through silicon carbide of relevant elements. Up to now we have investigated the transport of silver [3, 4], iodine [4, 5] and strontium [6]. The aim of this study is to obtain information on transport properties of cesium through silicon carbide at temperatures above 1000 °C and the influence of radiation damage on it. The isotope ^{137}Cs is one of the most hazardous fission products and is produced in relatively large quantities during nuclear burn-up. It is a β-emitter decaying to ^{137}Ba with a half-life of approximately 30 years, accompanied by energetic γ-radiation. It also is a major contaminant of radio-active fall-outs due to nuclear weapon tests or reactor accidents and can enter the human body via the food chain, where its biological half-life is 140 days in muscular tissue and 70 days in other parts of the body.

*Corresponding author, E mail: erich.friedland@up.ac.za

2. Experiment and Analysis

Hexagonal 6H-SiC from *Intrinsic Semiconductors*® and CVD-SiC from *Valley Design Corporation*®, having a columnar structure of mainly 3C-SiC crystallites, were used in this investigation. Cesium was implanted at 23 °C, 350 °C and 600 °C into the wafers with energy of 360 keV, a fluence of 10^{16} cm^{-2} and a flux not exceeding 10^{13} $cm^{-2}s^{-1}$. The implantation temperature was measured at the target holder close to the sample. According to simulations employing the TRIM-98 code [7] and assuming displacement energies of 35 eV for the silicon and 20 eV for the carbon atoms [8], the above fluence introduced maximum displacement damage of ~ 30 dpa at a depth of 72 nm. The different implantation temperatures made it possible to compare the evolution of transport processes in initially amorphous and crystalline silicon carbide. Diffusion was determined from the broadening of the implantation profiles after isochronal and isothermal annealing studies using RBS analysis. In the case of the single crystalline samples these measurements were combined with the results of α-particle channelling spectrometry to obtain defect density profiles as a function of implantation and annealing temperatures. Structural information on the samples before and after annealing was obtained by scanning electron microscopy. A detailed description of the experimental techniques used is given elsewhere [5].

To investigate the diffusion behaviour isochronal and isothermal annealing studies were performed. Fick's diffusion equation for the dilute limit leads to a particularly simple solution if the original profile at time $t_o = 0$ can be described by a Gaussian distribution [9]. In that case the concentration profile after annealing for a time t stays a normal distribution in an infinite medium and is given by

$$C(x,t) = K\,[\pi\, D\, t]^{-1/2}\, \exp(-x^2/4Dt).$$

In this equation K is an adjustable constant, while the position of the maximum concentration is unchanged at $x = 0$. Defining the profile width $W(t)$ as the full width at half maximum (FWHM), the following relationship between the final and original widths holds:

$$[W(t)]^2 = 4Dt\, \ln(2) + [W(0)]^2.$$

Hence, the diffusion coefficient D is directly obtained from the slope of a plot of $[W(t)]^2$ versus annealing time at constant temperature.

The as-implanted depth profiles at room and high temperatures display approximately a normal distribution. However, an increasing asymmetry is observed after high-temperature annealing when the diffusing atoms reach the surface. In order to exclude this surface effect from the analysis only data for depths of $d > 60$ nm are fitted to a Gaussian function. This exclusion also insures that the result is mainly determined by diffusion in the less damaged tail region of the distribution. As the shapes of the implantation profiles are nearly Gaussian in the peak region, this additional approximation should still allow an analysis in terms of the procedure discussed above without introducing too large uncertainties. Widths were obtained by applying the general fitting procedure of the GENPLOT code [10] to the Cs-peak of the RBS-spectra, which had been converted to a depth scale [5].

Results and Discussion

Fig. 1A shows the as-implanted RBS-channelling spectra of the cold and hot implants. The surface region of the cold implant is up to a depth of about190 nm totally amorphous, which only partly re-grows epitaxially from the bulk during annealing as illustrated in Fig.1B, while the remainder re-crystallizes into a finely grained polycrystalline phase. The implant at 350 ^{o}C exhibits a highly disordered buried layer from 25 to 180 nm below the surface, which, however, is not yet fully amorphous, as the single crystal lattice is restored after annealing. Apparently this temperature is just above the critical value for amorphization, which is significantly higher than observed for most other implantation species [11]. At an implantation temperature of 600 ^{o}C the crystal structure is retained, albeit with a high degree of distortions.

The cesium depth distributions at room temperature and at 600 °C are depicted in Fig 2 together with those of strontium [6] and iodine [5]. The broadening of the cesium profile at the higher implantation temperature of nearly 40% reveals an abnormally strong temperature dependence of irradiation induced diffusion. Less than 15% broadening is observed for the other two ion species. As iodine is almost as heavy as cesium, this dependence seems not to be directly related to the ion mass. Also shown are TRIM-98 simulations, which agree reasonably well as far as the projected ranges are concerned, but predict much smaller σ-values. In view of the many approximations made in this code, especially the neglect of thermal effects, this is not surprising.

Fig. 3 show isochronal annealing curves for the single and polycrystalline wafers. The as-implanted width of the 350 °C implantation is similar to that at room temperature in 6H-SiC, while it is more like the 600 °C implantation in CVD-SiC. It also appears that at 600 °C the width in the single crystalline sample is broadened more than in polycrystalline SiC, indicating that cesium might be more diffusive in the former material during implantation. However, in view of the relative large experimental uncertainties a definite conclusion cannot be drawn. In both samples the widths of the room temperature implants increase during the first annealing cycle due to diffusion in the initially amorphous surface regions. This does not occur in the samples implanted at 600 °C, where the basic crystal structure is retained. In the case of the 350 °C implants an increase of the width of the ion distribution is clearly observed in 6H-SiC, while this is not so obvious in CVD-SiC. Further width broadening occurs in all samples only at temperatures above 1200 °C. Within experimental errors, very little difference is observed for the six samples, although a slight tendency of less diffusion at higher implantation temperatures might be concluded from the 6H-SiC measurements. The retained cesium during isochronal annealing is depicted in Fig. 4. No loss occurs in both samples implanted at 600 °C, while approximately 50% is lost during the first annealing cycle in the samples implanted at room temperature. Obviously cesium diffuses relatively fast through the amorphous region towards the surface, where it evaporates into the vacuum. No further diffusion occurs after this first cycle, as the amorphous region recrystallizes simultaneously. A different behaviour is again observed for the 350 °C samples. The cesium loss in the single crystalline sample is similar to the cold implant, while only about 25% is lost from the polycrystalline sample. This, together with the results presented in Fig. 3 seems to indicate, that the degree of amorphization is less in the latter sample. However, whether this is due to the polycrystalline character cannot be decided with certainty from the results. From Fig. 1 it seems that the characteristic temperature for amorphization is near 350 °C for Cs implantation, which is higher than expected from a semi-empirical model [12, 13] but would be in accordance with values obtained for Ga and Sb ions implanted at similar energies [14,15]. At

this temperature the ion flux, which has not been closely monitored during implantation, can have a decisive influence on the degree of amorphization. The SEM-images displayed in Fig. 5 of these two samples after 5 hours annealing at 1100 °C prove that the CVD-wafer has still the original polycrystalline structure, while a finely grained structure is observed on the single crystalline wafer, which is typical for the early stages of re-crystallization of an amorphous surface region. During further annealing this feature disappears, indicating that sufficient information of the original crystal structure is still available for epitaxial re-growth.

Fig. 6 depicts isothermal annealing curves of the 6H-SiC wafers at 1200 ^{o}C, 1300 ^{o}C and 1400 ^{o}C. Similar curves are obtained with the CVD-SiC samples. The cold implants show the expected strong initial annealing before re-crystallization, but no further diffusion during subsequent annealing cycles. No diffusion at all, not even during the first cycle, is observed in the hot implants, which might be associated with the observed strong diffusion during implantation. Diffusion coefficients are obviously in all cases below our detection limit of 10^{-21} m^2 s^{-1}. This observation, which seems to be inconsistent with the relatively strong diffusion above 1200 ^{o}C during isochronal annealing, points to a trapping mechanism of impurities by defect structures. Diffusion processes are only taking place during periods of defect annealing and stop as soon as defect restructuring is coming to an end. Cesium atoms bound to defect complexes are released during their annihilation or restructuring, but are again captured after some time by more stable defects. During isochronal annealing that can happen after each cycle at a higher temperature, while during isothermal annealing it could only occur during the first cycle. A similar situation was also observed for the diffusion behaviour of strontium [6]. The retention of cesium during isothermal annealing displayed in Fig. 7 is the same as observed during isochronal annealing. No cesium loss from the hot implants and about 50% loss from the room temperature ones are found, while the samples implanted at 350 ^{o}C again report different losses of 50% and 25% from the 6H-SiC and CVD-SiC wafers respectively.

3. Conclusions.

An abnormally strong temperature dependence of irradiation induced diffusion is observed during cesium implantation compared with those of other ion species. This cannot easily be explained by an ion mass effect, as significantly less temperature dependence is observed for iodine, which is almost as heavy as cesium. Diffusion of cesium starts approximately at 1200 °C during isochronal annealing and is very similar in single and polycrystalline wafers up to temperatures of 1500 °C. However, isothermal annealing in this temperature range does not show any diffusion after prolonged heat treatment. This seemingly contradictory observation indicates that cesium transport in irradiation damaged SiC is governed by an impurity trapping mechanism, leading to negligible diffusion at constant temperatures up to at least 1400 ^{o}C. Our isochronal annealing results agree with those of Ref. [16], who observed that cesium diffusion after room temperature implantation started above 1150 °C.

4. Acknowledgements

Financial support of the *National Research Foundation* and the *Bundesministerium für Bildung und Forschung* is gratefully acknowledged. Thanks are due to Gerald Lenk from the *Institut für Festkörperphysik, Friedrich-Schiller-Universität Jena*, for the implantations.

5. References

[1] D. Hanson, A Review of Radionuclide Release from HTGR Cores During Normal Operation, Electric Power Research Institute, Report 1009382, March 2004.

[2] National Hydrogen Energy Roadmap, United States Department of Energy, Washington, DC, November 2002.

[3] E. Friedland, J.B. Malherbe, N.G. van der Berg, T Hlatshwayo, A.J Botha, E. Wendler, W. Wesch, J. Nucl. Mater. 389 (2009) 326.

[4] E. Friedland, N.G. van der Berg, J.B. Malherbe, R.J. Kuhudzai, A.J. Botha, E. Wendler, W. Wesch, Nucl. Instr.. and Meth. B 268 (2010) 2892.

[5] E. Friedland, N.G. van der Berg, J.B. Malherbe, J.J. Hanke, J. Barry, E. Wendler, W. Wesch, J. Nucl. Mater. 410 (2011) 24.

[6] E. Friedland, N.G. van der Berg, J.B. Malherbe, E. Wendler,. W. Wesch, J. Nucl. Mater. (2011); doi:10.1016/j.jnucmat.2011.10.032. (in press).

[7] J.F. Ziegler, J.P. Biersack, U. Littmark, "The Stopping and Ranges of Ions in Solids", Pergamon Press, New York (1985).

[8] R. Devanathan, W.J. Weber, F. Gao, J. Appl. Phys. 90 (2001) 2303.

[9] S.M. Myers, S.T. Picraux, T.S. Prevender, Phys. Rev. B 9 (1974) 3953.

[10] GENPLOT, Computer Graphics Service, (1989) Lansing, NY 14882.

[11] E. Wendler, A. Heft, W. Wesch, Nucl. Instr. and Meth. B 141 (1998) 105.

[12] W.J. Weber, Nucl. Instr. and Meth. B 166-167 (2000) 98.

[13] W.J. Weber, L. Wang, Y. Zhang, W. Jiang, I.-T, Bae, Nucl. Instr. and Meth. B 226 (2008) 2793.

[14] W. Wesch, A. Heft, E. Wendler, T. Bachmann, E. Glaser, Nucl. Instr. and Meth. B 96 (1995) 335.

[15] A. Heft, E Wendler, J. Heindl, T Bachmann, E. Glaser, H.P. Strunk, W. Wesch, Nucl. Instr. and Meth. B 113 (1996) 239.

[16] A. Audren, A. Benyagoub, L. Thomé, F. Garrido, Nucl. Instr. and Meth.B 257 (2007) 227.

Figure Captions

Fig. 1: RBS-channelling spectra of Cs-implants at different temperatures before (A) and after 10 hours annealing at 1200 °C (B).

Fig. 2: Depth profiles of strontium [6] (A), and iodine [5] (B) implanted at room temperature (X) and 600 °C (O) compared with those of cesium (C). The four distribution moments for the cold and hot implantations are given in each figure. Also shown are TRIM-98 simulations [7].

Fig. 3: Isochronal annealing curves for 6H-SiC (A) and CVD-SiC (B) at room temperature (O), 350 °C (X) and 600 °C (Δ).

Fig. 4: Retained cesium after 5 hours isochronal annealing of 6H-SiC (A) and CVD-SiC (B) implanted at room temperature (O), 350 °C (X) and 600 °C (Δ).

Fig. 5: SEM images of 6H-SiC (Top) and CVD-SiC (Bottom) implanted at 350 °C after 5 hours annealing at 1100 °C. The straight lines are polishing marks.

Fig. 6: Isothermal annealing curves of cold (A) and hot (B) implanted 6H-SiC at 1200 °C, 1300 °C and 1400 °C.

Fig. 7: Retained cesium in 6H-SiC (A) and CVD-SiC (B) implanted at room temperature (O), 350 °C (X) and 600 °C (Δ) after isothermal annealing at 1300 °C.

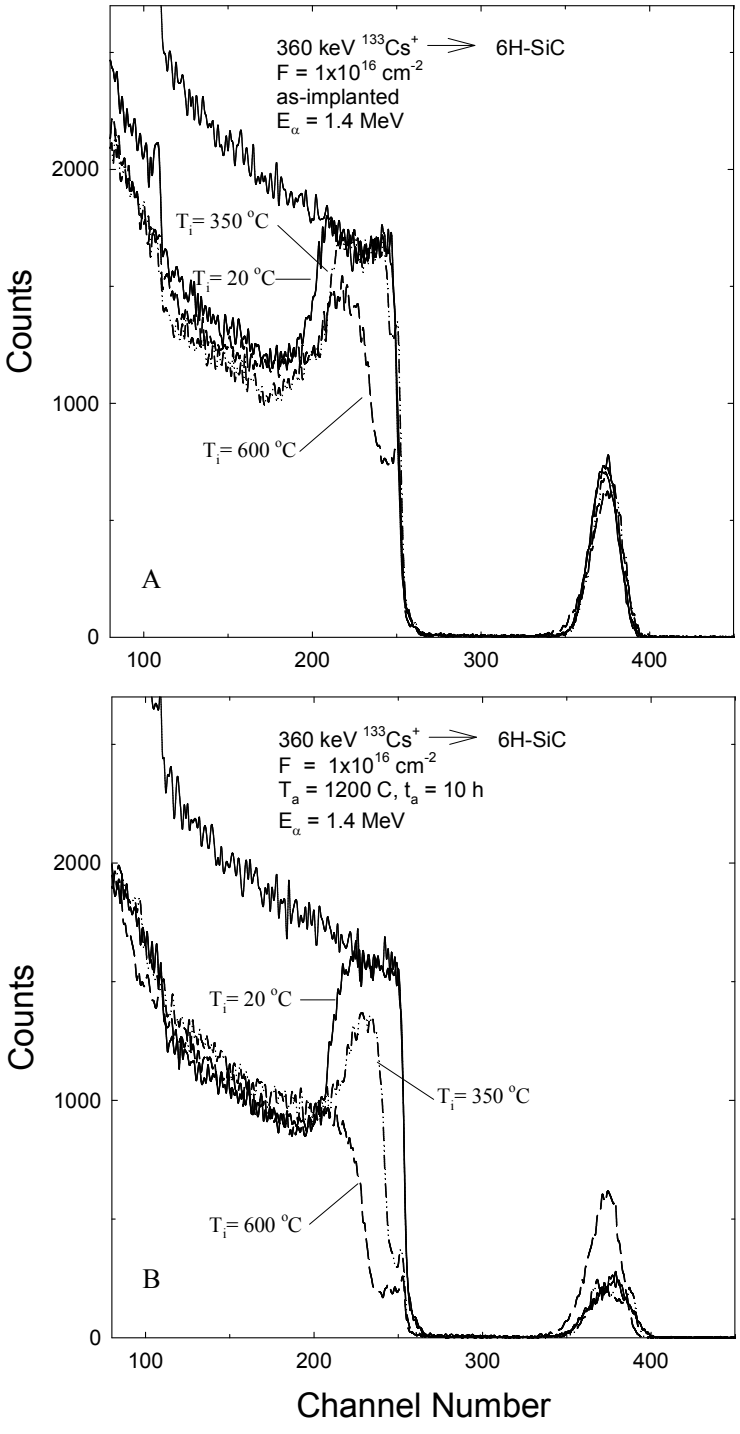
360 keV $^{133}Cs^+$ → 6H-SiC
F = 1x10^{16} cm^{-2}
as-implanted
E_α = 1.4 MeV
T_i= 350 °C
T_i= 20 °C
T_i= 600 °C
A
Counts
2000
1000
0
100
200
300
400
360 keV $^{133}Cs^+$ → 6H-SiC
F = 1x10^{16} cm^{-2}
T_a = 1200 C, t_a = 10 h
E_α = 1.4 MeV
T_i= 20 °C
T_i= 350 °C
T_i= 600 °C
B
Counts
2000
1000
0
100
200
300
400
Channel Number

Figure 1

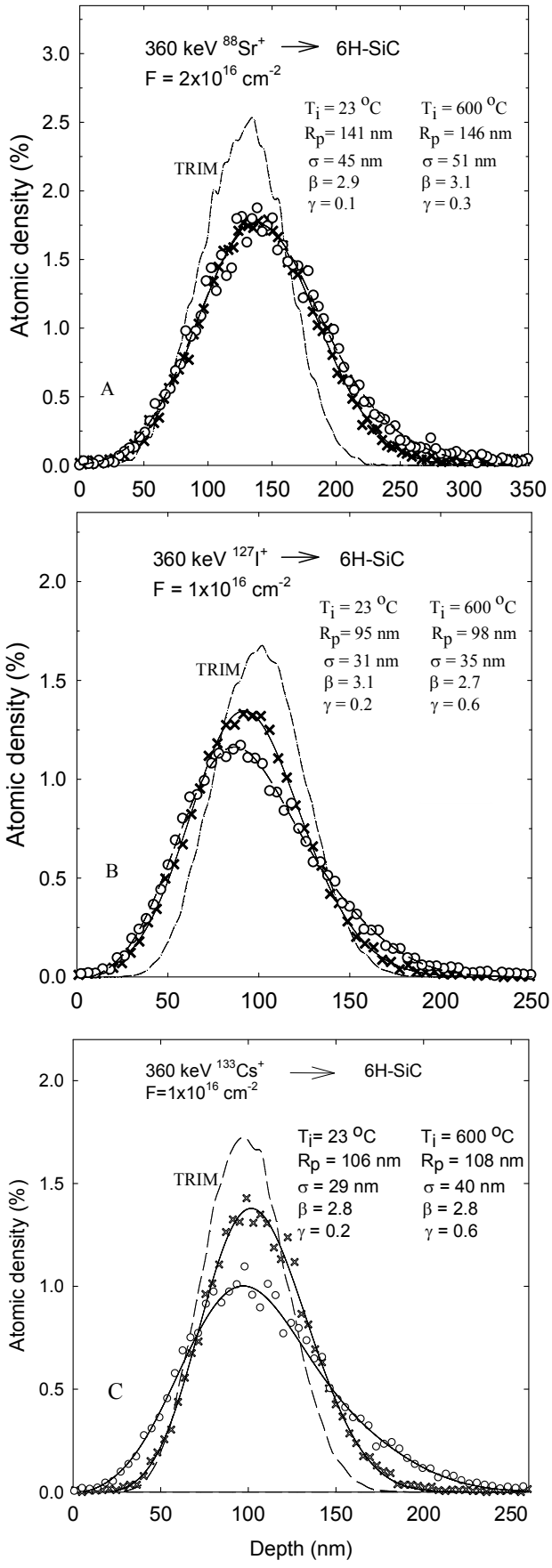
360 keV $^{88}Sr^{+}$ → 6H-SiC
F = 2x10^{16} cm^{-2}
T_i = 23 °C
R_p = 141 nm
σ = 45 nm
β = 2.9
γ = 0.1
T_i = 600 °C
R_p = 146 nm
σ = 51 nm
β = 3.1
γ = 0.3
TRIM
A
360 keV $^{127}I^{+}$ → 6H-SiC
F = 1x10^{16} cm^{-2}
T_i = 23 °C
R_p = 95 nm
σ = 31 nm
β = 3.1
γ = 0.2
T_i = 600 °C
R_p = 98 nm
σ = 35 nm
β = 2.7
γ = 0.6
TRIM
B
360 keV $^{133}Cs^{+}$ → 6H-SiC
F=1x10^{16} cm^{-2}
T_i= 23 °C
R_p = 106 nm
σ = 29 nm
β = 2.8
γ = 0.2
T_i = 600 °C
R_p = 108 nm
σ = 40 nm
β = 2.8
γ = 0.6
TRIM
C
Atomic density (%)
Depth (nm)

Figure 2

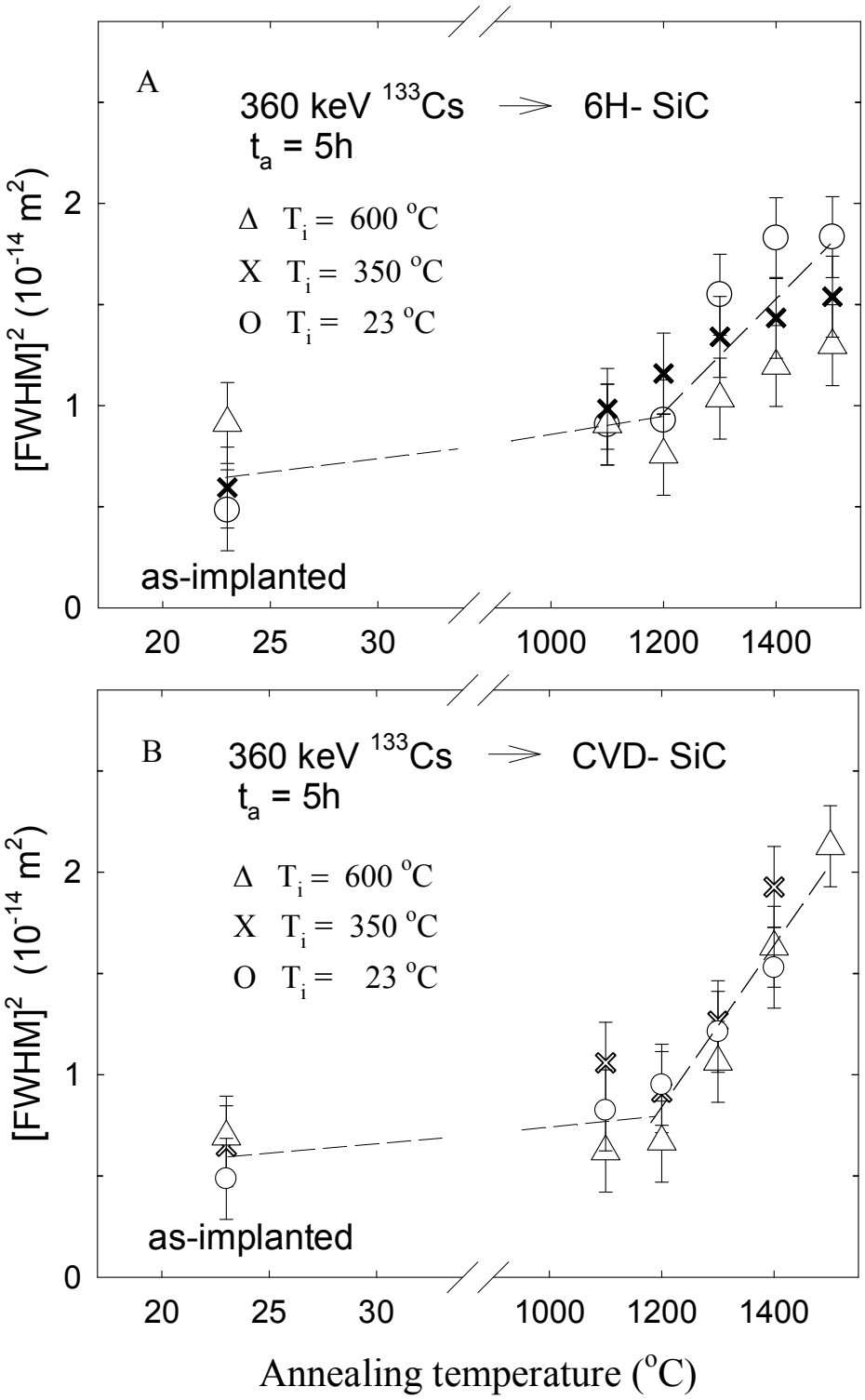
A
360 keV 133Cs → 6H- SiC
ta = 5h
Δ Ti = 600 °C
X Ti = 350 °C
O Ti = 23 °C
as-implanted
[FWHM]2 (10-14 m2)
B
360 keV 133Cs → CVD- SiC
ta = 5h
Δ Ti = 600 °C
X Ti = 350 °C
O Ti = 23 °C
as-implanted
[FWHM]2 (10-14 m2)
0
1
2
20
25
30
1000
1200
1400
Annealing temperature (°C)

Figure 3

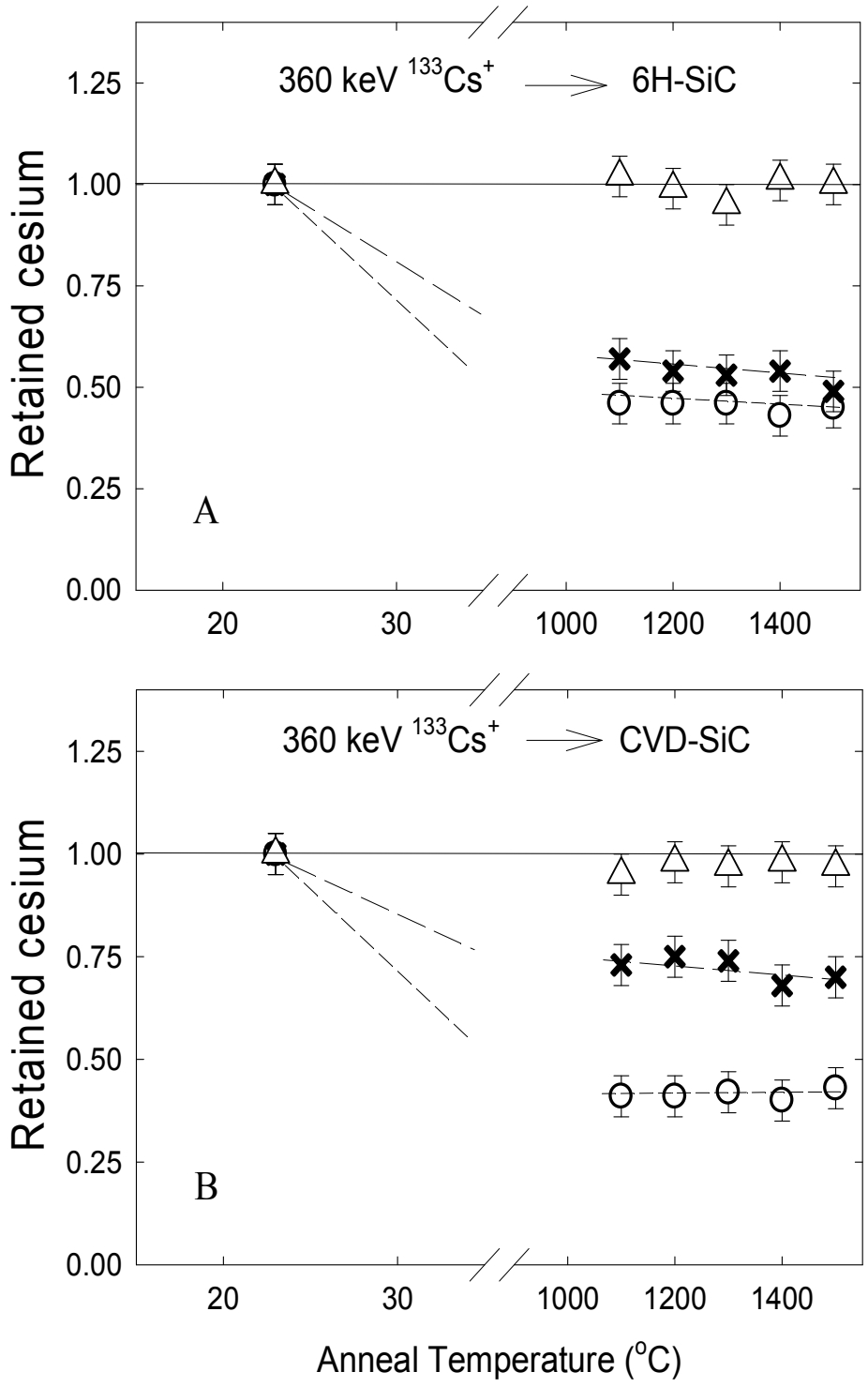
360 keV $^{133}Cs^{+}$ → 6H-SiC
Retained cesium
1.25
1.00
0.75
0.50
0.25
0.00
A
20
30
1000
1200
1400
360 keV $^{133}Cs^{+}$ → CVD-SiC
Retained cesium
1.25
1.00
0.75
0.50
0.25
0.00
B
20
30
1000
1200
1400
Anneal Temperature (°C)

Figure 4

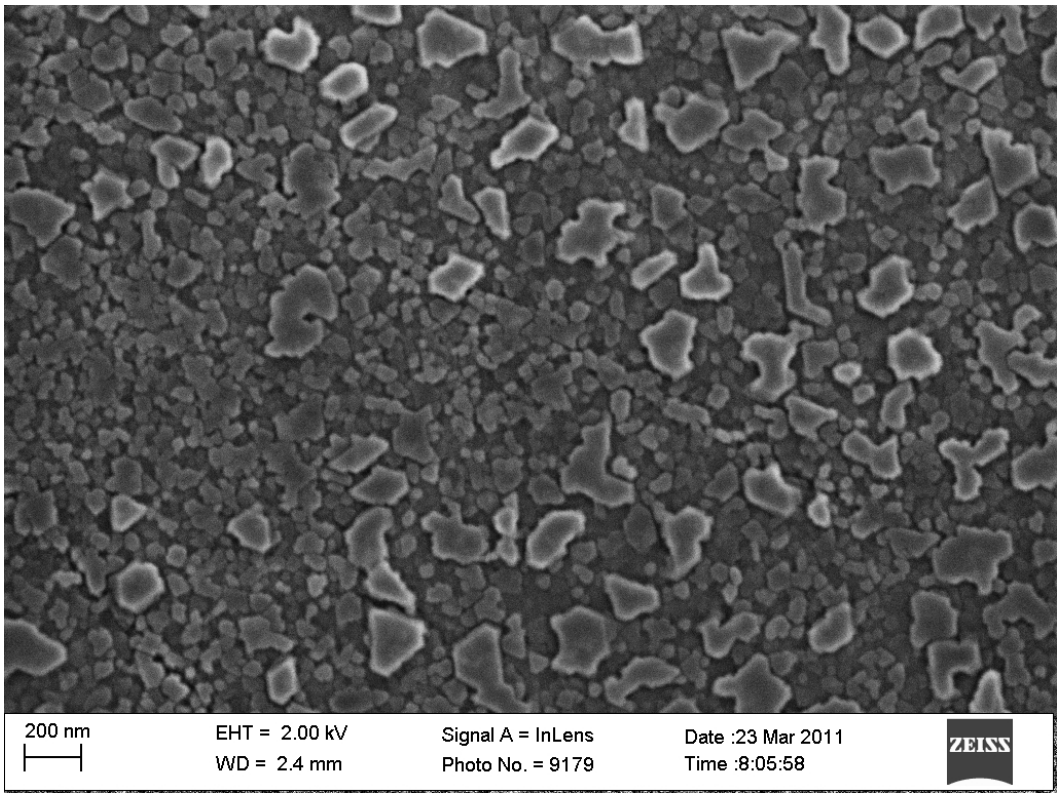
200 nm
EHT = 2.00 kV
WD = 2.4 mm
Signal A = InLens
Photo No. = 9179
Date :23 Mar 2011
Time :8:05:58
ZEISS

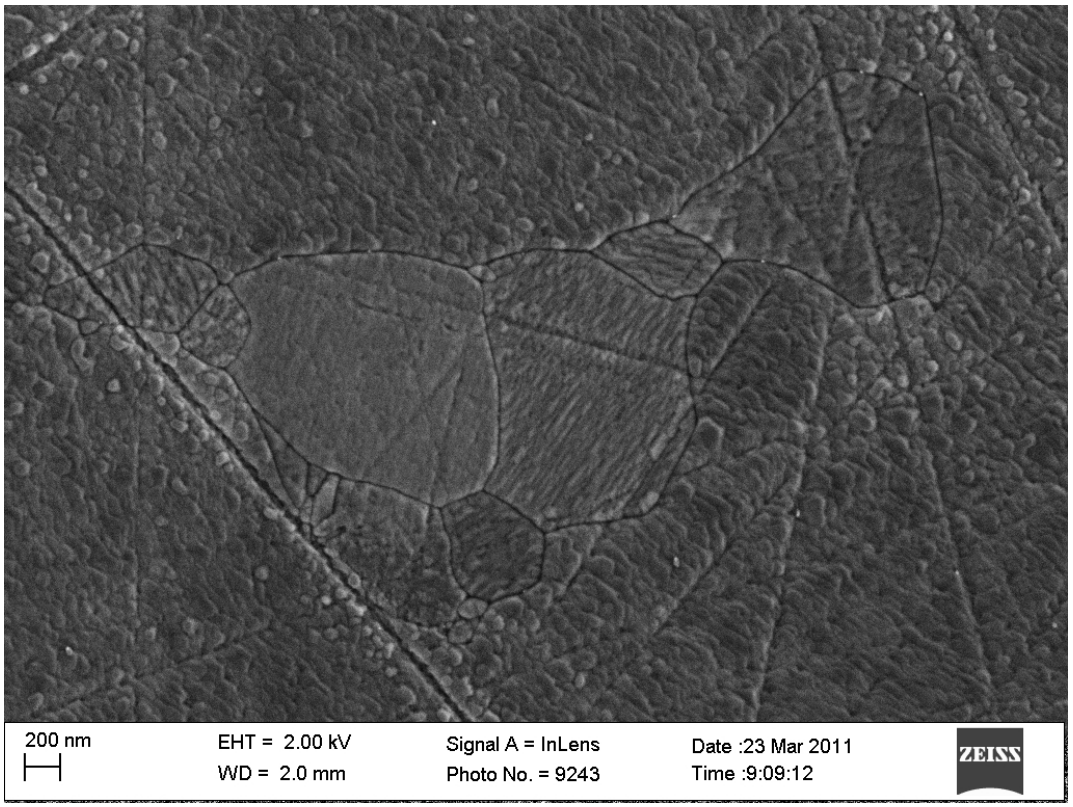
200 nm
EHT = 2.00 kV
WD = 2.0 mm
Signal A = InLens
Photo No. = 9243
Date :23 Mar 2011
Time :9:09:12
ZEISS

Figure 5

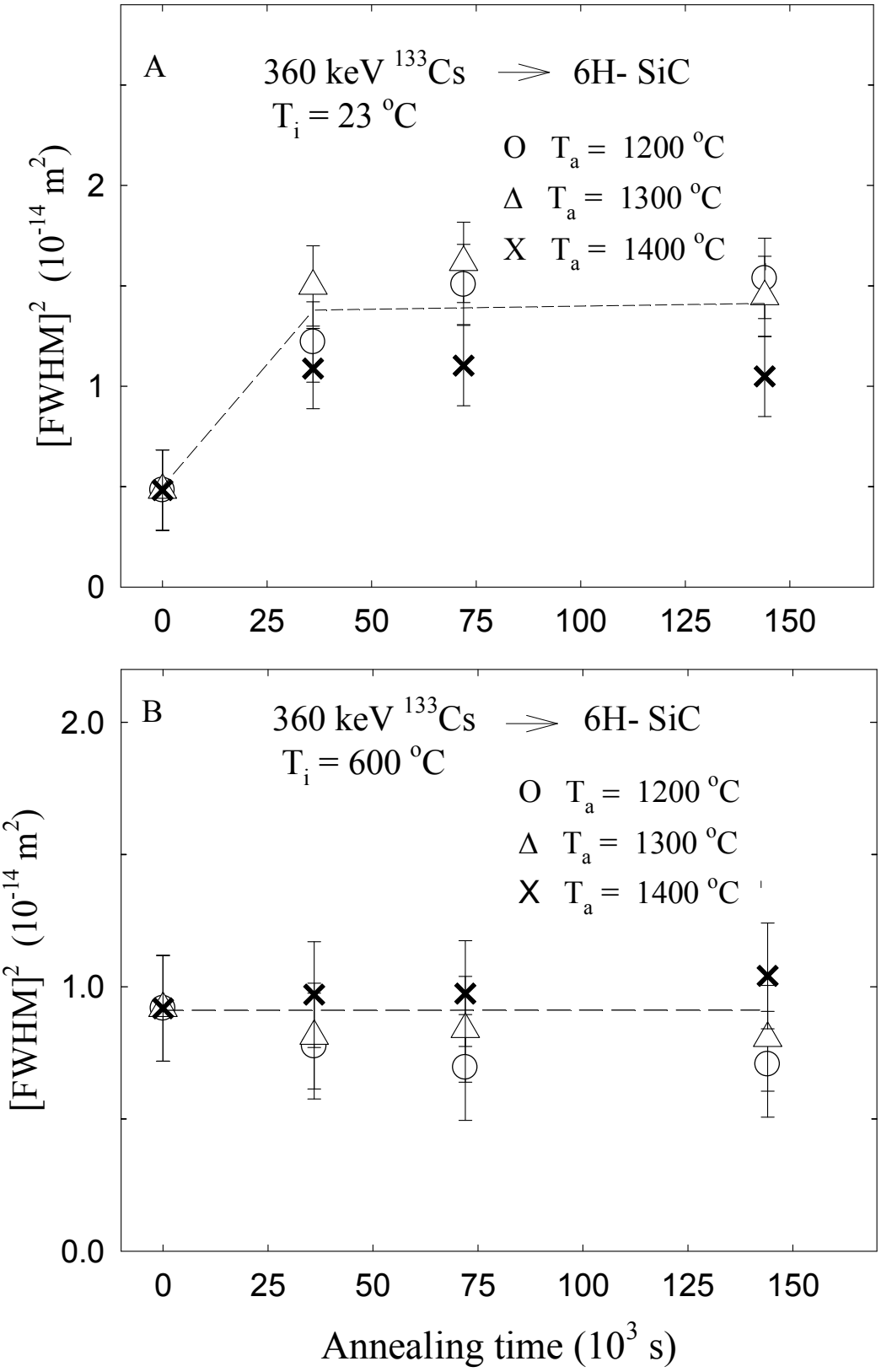
A
360 keV ^{133}Cs → 6H- SiC
T_i = 23 °C
O T_a = 1200 °C
Δ T_a = 1300 °C
X T_a = 1400 °C
[FWHM]^2 (10^{-14} m^2)
0
1
2
0
25
50
75
100
125
150
B
360 keV ^{133}Cs → 6H- SiC
T_i = 600 °C
O T_a = 1200 °C
Δ T_a = 1300 °C
X T_a = 1400 °C
[FWHM]^2 (10^{-14} m^2)
0.0
1.0
2.0
0
25
50
75
100
125
150
Annealing time (10^3 s)

Figure 6

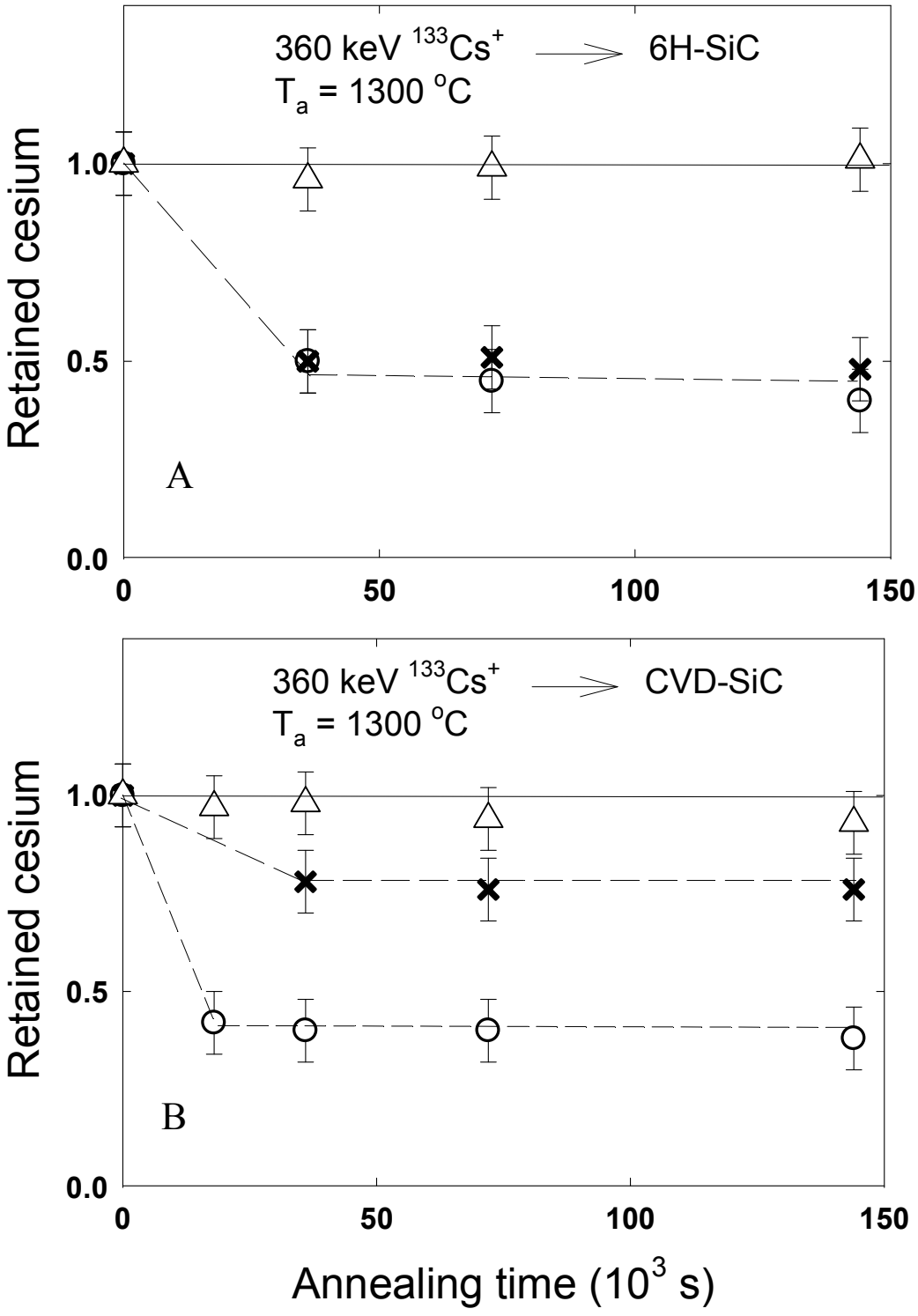
360 keV $^{133}Cs^+$ → 6H-SiC
T_a = 1300 °C
Retained cesium
1.0
0.5
0.0
A
0
50
100
150
360 keV $^{133}Cs^+$ → CVD-SiC
T_a = 1300 °C
Retained cesium
1.0
0.5
0.0
B
0
50
100
150
Annealing time (10^3 s)

Figure 7